Eddy-Current Loss Modeling for a Form-Wound Induction Motor Using Circuit Model

H. V. Khang and A. Arkkio

Department of Electrical Engineering, Aalto University, Espoo 02015, Finland

Eddy-current losses in a form-wound stator winding of a 1250-kW cage induction motor was modeled using time-discretized finite-element analysis (FEA). A simpler and faster model, typically a circuit model, is needed to include these losses in the loss control algorithms of a frequency converter. The conventional T-equivalent circuit was augmented by an additional branch both in the stator and rotor to model the eddy-current effects. The parameters of the refined circuit were estimated using the voltages and currents from the FEA simulations. The circuit model was verified by comparing the calculated losses and torque with those obtained from the FEA.

***Index Terms*—Eddy current, equivalent circuit, parameter estimation, skin effect.**

I. Introduction

ACCURATE prediction for eddy-current losses is essential when estimating the rated machine performance and temperature rise during the design stage [1]–[3]. Recently, FEA based methods have been proposed to model and reduce these losses [4], [5]. A loss-minimizing control of an electric drive typically utilizes a circuit model of the electric machine implemented in the control algorithms of the frequency converter [6]. A proper equivalent circuit with accurately estimated parameters is needed for an energy-efficient electric drive [7].

When applying time-discretized finite element analysis, it is relatively straightforward to identify linearized small-signal models for electrical machines [8]. These circuit models are based on the incremental reluctivity of the core material. The challenge is to find a relatively simple circuit model that represents the operating motor in several aspects. The current responses from the circuit have to be similar to those of the real motor. The skin effects, saturation, and core losses should be included. The model should be valid for both steady and transient states.

In the present paper, we propose a circuit model for a cage induction motor with form-wound stator winding. An augmented T-equivalent circuit is used. The parameters of the circuit are identified by a numerical approach and used to predict the losses and torque. The skin effect both in the stator and rotor winding is modeled. The magnetic saturation and core losses still remain a problem. The circuit parameters must be re-estimated if the flux of the machine is changed significantly. A good agreement between the circuit model and time-discretized FEA is shown by motor performance evaluations.

Manuscript received June 15, 2011; revised October 20, 2011; accepted October 20, 2011. Date of current version January 25, 2012. Corresponding author: H. V. Khang (e-mail: huynh.khang@aalto.fi).

Color versions of one or more of the figures in this paper are available online at http://ieeexplore.ieee.org.

Digital Object Identifier 10.1109/TMAG.2011.2173661

TABLE I
DATA OF MACHINE

Rated voltage (V)	690	Parallel strands in a coil	3
Rated Power (kW)	1250	Number of parallel branches	3
Rated slip (%)	0.365	Number of teeth in a coil pitch	10
Stator slots	72	Inner stator core diameter (mm)	670
Rotor slots	86	Outer rotor core diameter (mm)	663
Pole pairs	3	Effective length (mm)	810

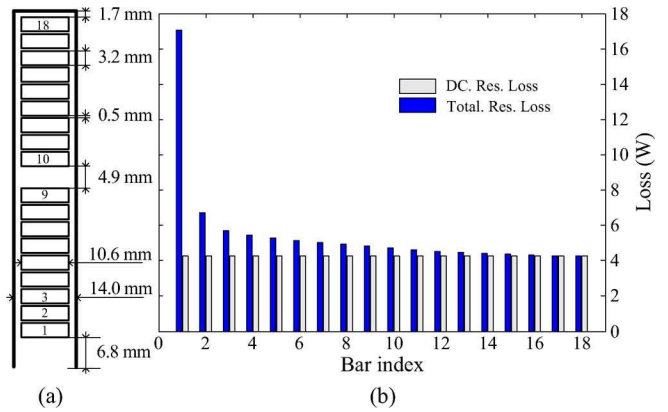

Fig. 1. (a) Stator winding and (b) its resistive loss distribution.

II. Eddy Current Losses in the Stator Windings

A method to model eddy current losses in a form-wound stator winding of an IM was presented in [5]. The eddy-current loss P_{eddy} is the difference between the total resistive loss P_{t} and dc resistive loss:

$$P_{\mathrm{eddy}} = P_{\mathrm{t}} - \sum_{j=1}^{m} R_{\mathrm{dc}} i_j^2 \tag{1}$$

where i_j is the phase current in stator phase j, R_{dc} is the dc resistance of a phase, and m is the number of the phase.

The basic data of the motor studied is shown in Table I. As recommended from previous researches, the stator winding of the motor is shown in Fig. 1(a), in which a distance 6.8 mm from the inner stator surface to the first stator bar hsb is selected in order to satisfy the standard IEC 60034-1 [5]. The parameters of

TABLE II
T-EQUIVALENT CIRCUIT PARAMETERS USING TIME-HARMONIC FEA

R_s (Ω)	$L_{\sigma s}$ (H)	L_m (H)	R_r (Ω)	L_r (H)
5.53E-03	2.82E-04	7.05E-03	3.63E-03	2.72E-04

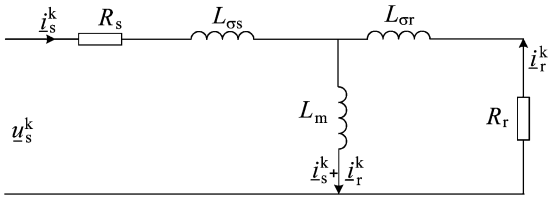

Fig. 2. Traditional IM equivalent circuit.

the traditional T-circuit model estimated using time-harmonic FEA [9] are shown in Table II. The resistive-loss distribution in the stator bars is presented in Fig. 1(b). Fig. 1(b) indicates that using a simple dc resistance cannot model the eddy-current losses of the stator windings. The current or loss density is not homogeneous over the cross section of the bar. A similar phenomenon also occurs in semi-open rotor slots. In addition to the fundamental component, the induced currents in the bars contain many other harmonics, for instance, the stator slot harmonics in the moving rotor.

A Cauer circuit seems to be the most straightforward approach to model the skin effect or eddy currents in a conductor [10], [11]. The Cauer ladder model is also applied for the present study. Stator voltages and currents obtained from the time-discretized FEA are used as the data for parameter estimation. The performance of the motor simulated by FEA will be compared with the result from the circuit model.

III. EQUIVALENT CIRCUIT MODELS

A. T-Equivalent Circuit

The conventional T-circuit model for the IM shown in Fig. 2 includes the stator and rotor leakage inductances $L_{\sigma s}$ and $L_{\sigma r}$; magnetizing inductance L_m; stator resistance R_s; and rotor resistance R_r. The voltage and flux equations in a reference frame rotating at speed ω_k are written in the space-vector form for control purposes:

$$\underline{u}_s^k = R_s \underline{i}_s^k + \frac{d\underline{\psi}_s^k}{dt} + j\omega_k \underline{\psi}_s^k \tag{2}$$

$$\underline{u}_r^k = R_r \underline{i}_r^k + \frac{d\underline{\psi}_r^k}{dt} + j(\omega_k - \omega_0)\underline{\psi}_r^k \tag{3}$$

$$\underline{\psi}_s^k = (L_m + L_{\sigma s})\underline{i}_s^k + L_m \underline{i}_r^k \tag{4}$$

$$\underline{\psi}_r^k = L_m \left(\underline{i}_s^k + \underline{i}_r^k\right) + L_{\sigma r} \underline{i}_r^k \tag{5}$$

and ω_0 is the rotor speed.

The small-signal impedance of the motor in the stator reference frame ($\omega_k = 0$) can be derived by studying small disturbances in voltages, currents, and flux linkages (2)–(5) in Laplace domain:

$$Z_e = \frac{\underline{Z}_s(\underline{Z}_m + \underline{Z}_r) + \underline{Z}'_m \underline{z}_r}{\underline{Z}_m + \underline{Z}_r} = \frac{\Delta \underline{u}_s}{\Delta \underline{i}_s} \tag{6}$$

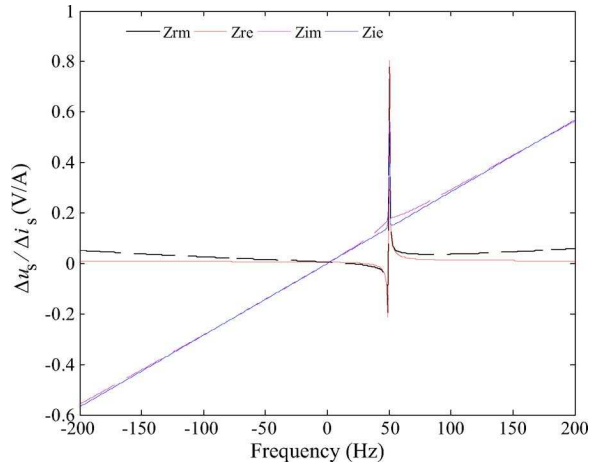

Fig. 3. Frequency response of T model.

where

$$\underline{z}_s(s) = sL_{\sigma s} + R_s \tag{7}$$

$$\underline{z}_m(s) = sL_m - j\omega_0 L_m \tag{8}$$

$$\underline{z}'_m(s) = sL_m \tag{9}$$

$$\underline{z}_r(s) = R_r + sL_{\sigma r} - j\omega_0 L_{\sigma r}. \tag{10}$$

The parameters are estimated by minimizing the error between the simulated frequency response function (FRF) and the FRF given by the analytical model (6). The cost function is defined as

$$I = \sum_{n=1}^{N} \left[\left(\mathrm{Re}\{Z_m^n\} - \mathrm{Re}\{Z_e^n\}\right)^2 + \left(\mathrm{Im}\{Z_m^n\} - \mathrm{Im}\{Z_e^n\}\right)^2 \right]. \tag{11}$$

N is the length of vector data, n is the sample index, Z_m is the FRF obtained from the impulse method, and Z_e is the FRF from the circuit model (6). All small-signal data are extracted from two time-discretized FEA simulations. In the first one, the fundamental input signal (u_s) and impulse input signal (Δu_s) are applied and, thus, the current response includes two components as well, i_s and Δi_s. In the latter simulation, only the fundamental signal (u_s) is applied.

The Differential Evolution method is used to estimate the parameters. This method can minimize the nonlinear and nondifferentiable continuous function (11). It is fast, simple, and effectively global optimized. The details of the method are described in [12].

The best fit between the data from FEA and circuit model is shown in Fig. 3. There is a large deviation between those FRFs both in small and large range of frequencies. It is reconfirmed that the T-circuit model could not suffice to describe the behavior of the motor. A more advanced circuit is required to include the skin or eddy-current effects.

B. Proposed Circuit

The motor with semi-open rotor slots and form-wound stator winding is modeled by using additional branches as shown in Fig. 4. R_e and L_{se} stand for the stator eddy-current effect. R_{r2} and L_{r2} are added for the skin effect of the semi-open rotor slots.

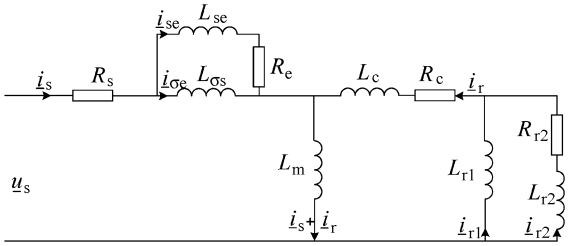

Fig. 4. Equivalent circuit for the form-wound IM.

The mathematical meaning of the extra Cauer ladders is that they increase the order of the impedance FRF.

The small-signal impedance of motor (6) is still valid for the circuit in Fig. 4, but the stator and rotor impedances of the circuit are changed as follows:

$$\underline{z}_s(s) = R_s + \left(\frac{1}{sL_{\sigma s}} + \frac{1}{R_e + sL_{se}}\right) \tag{12}$$

$$\underline{z}_r(s) = R_c + (s - j\omega_0)L_c + \left(\frac{1}{(s - j\omega_0)L_{r1}} + \frac{1}{R_{r2} + (s - j\omega_0)L_{r2}}\right). \tag{13}$$

The stator flux becomes

$$\underline{\psi}_s = L_{\sigma s}\underline{i}_{\sigma s} + L_{se}\underline{i}_{se} + L_m(\underline{i}_{r1} + \underline{i}_{r2} + \underline{i}_{\sigma s} + \underline{i}_{se}). \tag{14}$$

The voltages and currents of the motor are obtained from several time-discretized FEA simulations. First, the effect of saturation is neglected by using a relative permeability of 1000 for the iron (referred to as a linear case). The machine is simulated twice, first modeling the stator eddy currents and then without the eddy currents by using constant current density. Next, the permeability is allowed to change according to the flux density (a nonlinear case). Again, the machine is modeled with and without the stator eddy currents. As recommended in [12], to eliminate the anisotropy related to magnetic saturation, the average impedance from two impulse tests is used to estimate the circuit parameters in the nonlinear case. The two impulse signals have angles 0 and 90° with respect to the steady-state voltage vector.

Fig. 5 shows the best fit for the data between the time-discretized FEA and the proposed circuit for the nonlinear case when the eddy-current effects in stator winding are included as well. The proposed circuit gives a very good agreement between the impedance FRF and the collected data.

The parameters estimated for the studied cases are listed in Table III. The dc stator resistance is easily determined for the rated temperature and fixed to that value. One simple way to verify the circuit is to supply the circuit with the voltage that is used in the FEA as shown in Fig. 6. The current response from the circuit has to be similar to that obtained from the FEA. Fig. 7 shows the stator current response of the FEA and circuit model at rated load for the nonlinear case including the stator eddy-current effect. It is clear that the stator current response from the circuit fits well the stator current response from FEA for both amplitude and phase.

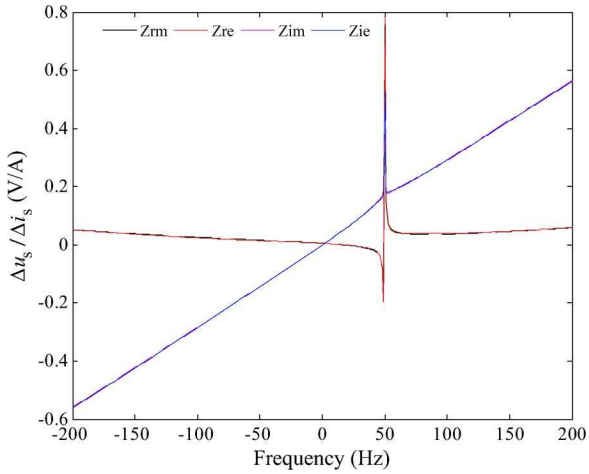

Fig. 5. Frequency response of the proposed model.

TABLE III
PARAMETERS ESTIMATED FOR THE CIRCUIT MODEL

	Linear		Nonlinear	
	without stator eddy current	including stator eddy current	without stator eddy current	including stator eddy current
R_s (Ω)	5.53E-03	5.53E-03	5.53E-03	5.53E-03
$L_{\sigma s}$ (H)	1.64E-04	1.84E-04	1.79E-04	1.49E-04
R_e (Ω)	1.328E+0	1.382E+0	1.595E+0	0.925E+0
L_{se} (H)	1.50E-04	1.05E-04	1.90E-04	3.42E-05
L_m (H)	6.61E-03	6.77E-03	6.22E-03	6.83E-03
R_c (Ω)	3.82E-03	3.75E-03	3.82E-03	3.83E-03
L_c (H)	5.78E-06	1.32E-05	2.87E-05	1.32E-05
L_{r1} (H)	3.75E-04	3.54E-04	3.32E-04	3.91E-04
R_{r2} (Ω)	2.17E-01	1.92E-01	1.77E-01	2.40E-01
L_{r2} (H)	1.26E-03	1.10E-03	1.10E-03	1.37E-03

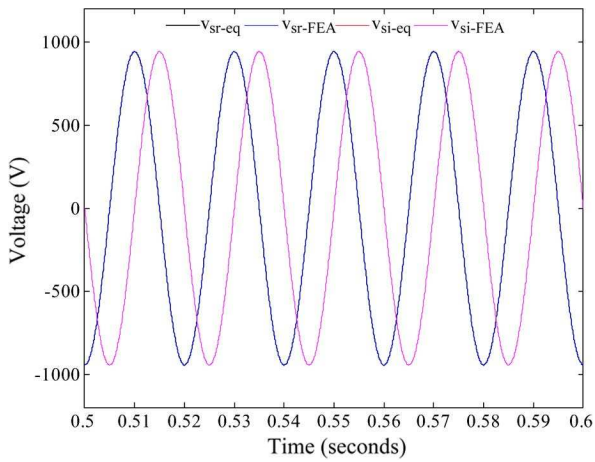

Fig. 6. Space-vector components of voltage supply.

C. Performance Evaluation

The motor performance predicted by the proposed circuit model is discussed in this section. The electromagnetic torque is calculated as follows:

$$T_{eq} = \frac{3}{2}p\mathrm{Im}\left\{\underline{\psi}_s^* \underline{i}_s\right\} \tag{15}$$

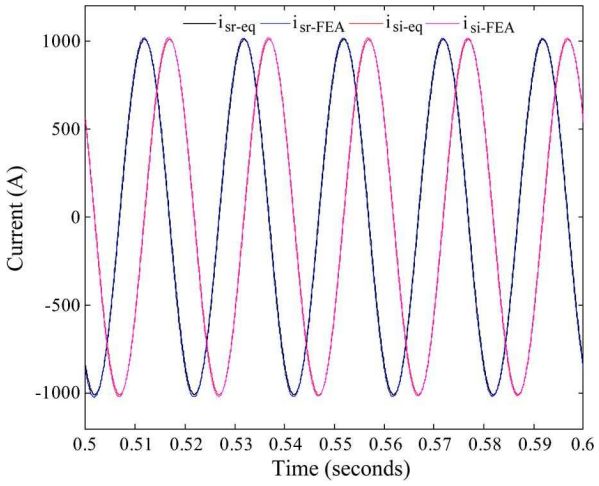

Fig. 7. Space-vector components of stator current response.

TABLE IV
LOSSES AND TORQUE FROM FEA AND CIRCUIT MODEL

	Linear		Nonlinear	
	without stator eddy current	including stator eddy current	without stator eddy current	including stator eddy current
T_{eq} (N.m)	11184	11326	11101	11228
T_{FEA}(N.m)	11381	11382	11432	11429
error (%)	-1.73	-0.49	-2.90	-1.76
P_{eq} (W)	15817	16626	15934	16284
P_{FEA}(W)	15427	16195	15579	16059
error (%)	2.53	2.66	2.28	1.4

where the stator flux $\underline{\Psi}_{\rm s}$ is computed from (14) by using the circuit parameters.

The total resistive loss of the motor is

$$P_{\rm eq} = \frac{3}{2}\left(R_{\rm s}I_{\rm s}^2 + R_e I_e^2 + R_{\rm c}I_r^2 + R_{\rm r2}I_{\rm r2}^2\right) \qquad (16)$$

where $I_{\rm s}$, $I_{\rm e}$, $I_{\rm r}$, and $I_{\rm r2}$ are the rms values of the $\underline{i}_s$, $\underline{i}_e$, $\underline{i}_r$, and $\underline{i}_{r2}$ in Fig. 4.

Table IV lists the torque $T_{\rm eq}$ and total loss $P_{\rm eq}$ calculated from the proposed circuit and those from the time-discretized FEA as presented in Section II ($T_{\rm FEA}$ and $P_{\rm FEA}$). The relative errors of the torque or total loss are defined by

$$\text{error}_X(\%) = \frac{X_{\rm eq} - X_{\rm FEA}}{X_{\rm FEA}} 100\% \qquad (17)$$

where X is either the torque or total loss.

A suitable circuit model and well estimated parameters are able to predict the performance of the motor. The maximum error is less than 3% for all studied cases.

When the motor is fed by a frequency converter, the supply voltage is highly distorted by harmonics. The control algorithm of the converter needs a circuit model, which is valid over a wide range of frequencies. The circuit model proposed is valid for -200 Hz to 200 Hz (Fig. 5) and has constant parameters. Therefore, the model does not only represent the motor well, but is also simple to implement to the motor control algorithm.

IV. CONCLUSION

The circuit model proposed for an inverter-fed form-wound IM was well identified by using FEA data. It is shown that an appropriate circuit model is able to predict the performance of the motor very accurately when compared to time-discretized FEA. The proposed circuit can take the eddy-current effect into account and predict well resistive losses of the motor for control purposes. Inclusion of iron losses to the circuit is a subject for future studies.

ACKNOWLEDGMENT

The authors would like to acknowledge Dr. A.-K. Repo, Konecranes Plc, and Dr. M. J. Islam, ABB Sweden, for their co-operation. The authors gratefully acknowledge the financial of the Academy of Finland; the School of Electrical Engineering, Aalto University; the Fortum Foundation; the Finnish Cultural Foundation; and the Association of Electrical Engineers in Finland.

REFERENCES

[1] N. Kunihiro, T. Todaka, and M. Enokizono, "Loss evaluation of an induction motor model core by vector magnetic characteristic analysis," *IEEE Trans. Magn.*, vol. 47, no. 5, pp. 1098–1101, 2010.

[2] Y. Amara, P. Reghem, and G. Barakat, "Analytical prediction of Eddy-current loss in armature windings of permanent magnet brushless AC machines," *IEEE Trans. Magn.*, vol. 46, no. 8, pp. 3481–3484, 2010.

[3] L. Ruifang, C. C. Mi, and D. W. Gao, "Modeling of Eddy-current loss of electrical machines and transformers operated by pulsewidth-modulated inverters," *IEEE Trans. Magn.*, vol. 44, no. 8, pp. 2021–2028, 2008.

[4] K. Yamazaki, M. Shina, Y. Kanou, M. Miwa, and J. Hagiwara, "Effect of Eddy current loss reduction by segmentation of magnets in synchronous motors: Difference between interior and surface types," *IEEE Trans. Magn.*, vol. 45, no. 10, pp. 4756–4759, 2009.

[5] M. J. Islam, H. V. Khang, A.-K Repo, and A. Arkkio, "Eddy-current loss and temperature rise in the form-wound stator winding of an inverter-fed cage induction motor," *IEEE Trans. Magn.*, vol. 46, no. 8, pp. 3413–3416, 2010.

[6] A. M. Bazzi and P. T. Krein, "Review of methods for real-time loss minimization in induction machines," *IEEE Trans. Ind. Appl.*, vol. 46, no. 6, pp. 2319–2328, 2010.

[7] J. Corda and S. M. Jamil, "Experimental determination of equivalent-circuit parameters of a tubular switched reluctance machine with solid-steel magnetic core," *IEEE Trans. Ind. Electron.*, vol. 57, no. 1, pp. 304–310, 2010.

[8] A. Repo and A. Arkkio, "Numerical impulse response test to estimate circuit-model parameters for induction machines," in *Proc. Inst. Elect. Eng.—Electric Power Appl.*, 2006, vol. 153, no. 6, pp. 883–890.

[9] A.-K. Repo, A. Niemenmaa, and A. Arkkio, "Estimating circuit models for a deep-bar induction motor using time harmonic finite element analysis," presented at the Int. Conf. Electrical Mach., Crete, Greece, Sep. 2006.

[10] J. H. Krah, "Optimum discretization of a physical Cauer circuit," *IEEE Trans. Magn.*, vol. 41, no. 5, pp. 1444–1447, 2005.

[11] J. L. Guardado, J. A. Flores, V. Venegas, J. L. Naredo, and F. A. Uribe, "A machine winding model for switching transient studies using network synthesis," *IEEE Trans. Energy Convers.*, vol. 20, no. 2, pp. 322–328, 2005.

[12] A.-K. Repo, "Numerical impulse response tests to identify dynamic induction-machine models" Ph.D. Sci.Tech. dissertation, Helsinki Univ. of Technol., Helsinki, Finland, 2008 [Online]. Available: http://lib.tkk.fi/Diss/2008/isbn9789512292752/